The expression profile of developmental stage-dependent circular RNA in the immature rat retina

Junde Han, Lingqi Gao, Jing Dong, Jie Bai, Mazhong Zhang, Jijian Zheng

Shanghai Children's Medical Center, Shanghai Jiao Tong University School of Medicine, Shanghai, China

Purpose: Physiologic neuronal apoptosis, which facilitates the developmental maturation of the nervous system, is regulated by neuronal activity and gene expression. Circular RNA (circRNA), a class of non-coding RNA, regulates RNA and protein expression. As the relationship between circRNA and apoptosis is unknown, we explored changes in expression patterns of circRNA during physiologic neuronal apoptosis.
Methods: High-throughput sequencing was used to explore changes in the expression of circRNA in the postnatal developing rat retina. Neuronal apoptosis was determined with immunohistochemistry and terminal deoxynucleotidyl transferase dUTP nick end labeling (TUNEL) in the rat retinal ganglion cell layer.
Results: In total, 2,654, 7,201, and 5,628 circRNA species were detected in the postnatal day (P)3, P7, and P12 rat retina, respectively. Of these circRNA species, 1,371 changed statistically significantly between P3 and P7 and 1,112 changed statistically significantly between P7 and P12. Normal developmental apoptosis, measured with the ratio of apoptotic (caspase-3- or TUNEL-positive) cells to normal cells, showed an increase from P3 to P7 and then a reduction from P7 to P12. In addition, 15 circRNAs whose host genes were associated with apoptosis were differentially expressed during the early development period.
Conclusions: These results associate circRNAs with neuronal apoptosis, providing potential mechanisms and treatment targets for physiologic and drug-induced apoptosis in the developing nervous system.

During the period of synaptic formation and refinement, especially at the peak of synaptogenesis, many neuronal cells undergo apoptosis, or programmed cell death (PCD, also called physiologic apoptosis), to ensure the establishment of accurate neuronal connections and networks [1-4]. In the rodent brain, this process mainly occurs within the 2 weeks after birth, primarily during postnatal days 4 to 14 (P4–P14) [5,6]. The nervous system is also vulnerable to ethanol, general anesthetics, and other substances during this period [7,8]. The underlying mechanism regulating the neuronal apoptotic process remains unclear, but numerous studies demonstrate that neuronal activity and genetic modulation play highly significant roles.

In the developing rat retina, the peak of physiologic apoptosis coincides with the transition from early cholinergic-driven, synchronized spontaneous network activity to glutamatergic-driven activity [9,10]. Blockade of this neural activity by ketamine during this transition period aggravates physiologic apoptosis [11]. During this transition, some relevant receptors, signaling pathways, and apoptosis-related genes also experience dramatic changes [10,12-15]. Previous

studies on mRNA or transcription factors to cleave or down-regulate mRNA have shown that noncoding microRNA (miRNA) species are involved in neurogenesis, proliferation, axon extension (e.g., mir-9) [16,17], and neuronal apoptosis (e.g., mir-21, -23, -26, -27, and -29) [18-21].

Circular RNA (circRNA), formed by back-splicing, has been reported for decades because of splicing errors [22,23]. More recently, studies have shown that circRNAs are expressed in a variety of eukaryotic organisms, including mammals, and are involved in various physiologic or pathological processes. CircRNAs are widely expressed and show temporal and spatial changes during development [24-27]. This large class of RNA has regulatory abilities, acting as protein or miRNA "sponges" and regulating mRNA transcription or translation [28,29]. Recent studies have shown that circRNAs are remarkably enriched in the nervous system, especially in synapses, during development; circRNAs were also found to regulate synaptic function and neuronal plasticity [30,31]. However, the relationship between circRNAs and physiologic neuronal apoptosis is largely unknown.

Development-related neuronal apoptosis in the central nervous system of rodents mainly occurs within 2 weeks after birth and peaks at about P7 [11]. Thus, we chose to analyze the rat retina at the P3, P7, and P12 time points, to determine any possible associations between physiologic neuronal

Correspondence to: Jijian Zheng, Department of Anesthesiology, Shanghai Children's Medical Center, Shanghai Jiao Tong University School of Medicine, Shanghai, China 1678 Dongfang Road, Pudong, Shanghai, China, Zip code: 200127; Phone: +86(21) 38626161; FAX: +86(021) 58393915; email: zhengjijian626@sina.com

apoptosis and changes in the expression of circRNA during postnatal development.

METHODS

Animals and tissue dissection: Sprague-Dawley rat pups (male and female) aged P3, P7, and P12 days were provided by the Experimental Animal Center at the Shanghai General Hospital in Shanghai, China. Eight rat pups were used for each group of P3, P7, and P12. Rat pups were housed with their dam under a 12 h:12 h light-dark cycle at room temperature 35–37 °C, with food and water available ad libitum until the experiments were conducted. All experimental procedures were reviewed and approved by the Animal Care Committee at the Shanghai General Hospital, Shanghai Jiao Tong University School of Medicine, and were conducted under the guidelines of the Care and Use of Laboratory Animals published by the U.S. National Institutes of Health (National Institutes of Health Publication No. 85–23, revised in 1996) and the ARVO Statement for the Use of Animals in Ophthalmic and Vision Research. Every effort was made to minimize the number of animals used, and their discomfort, during all experimental procedures.

Because of the limited size of the rat retina, we combined the retinas of each group of P3, P7, and P12 rats for high-throughput sequencing of circRNA and immunohistochemistry or terminal deoxynucleotidyl transferase dUTP nick end labeling (TUNEL) assay. The basic experimental protocol was slightly modified from that in previous studies [32]. Briefly, the pups were euthanized instantaneously by decapitation, and then their eyes were rapidly dissected with fine scissors and transferred to an ice-cold (0–4 °C) bath of artificial cerebrospinal fluid (ACSF: composition in mM: NaCl 119, KCl 2.5, K_2HPO_4 1.0, $CaCl_2$ 2.5, $MgCl_2$ 1.3, $NaHCO_3$ 26.2, and D-Glucose 11). The bath was continuously bubbled with a 95% O_2/5% CO_2 gas mixture. About one fifth of the eyeball circumference at the edge of the cornea and sclera was resected using ophthalmological scissors to facilitate the perfusion of ACSF through the retina. After 1 h of recovery in ACSF (37 °C) bubbled with a 95% O_2/5% CO_2 gas mixture, the retinas were dissected and then either frozen quickly with liquid nitrogen for circRNA high-throughput sequencing or fixed in 4% paraformaldehyde at 4 °C for 24 h for immuno-histochemistry and the TUNEL assay.

Cleaved caspase-3 immunohistochemistry and TUNEL: After the retinas were embedded in paraffin, retinal sections of 4 µm thickness were prepared. Three percent hydrogen peroxide was used to inactivate endogenous peroxidases, and EDTA, adjusted to pH 9.0, was used for heat-induced antigen retrieval for 8–10 min. After rinsing with PBS (1X; 137 mM NaCl, 2.7 mM KCl, 10 mM Na_2HPO_4, 2 mM KH_2PO_4, pH 7.4), retinal sections were incubated with rabbit anti-cleaved caspase-3 primary antibody (#9661s, dilution: 1/300, Cell Signaling Technology, Danvers, MA) was performed at 4 °C overnight, followed by incubation with goat anti-rabbit immunoglobulin G (IgG; PV-9001, ZSGB-BIO, Beijing, China) secondary antibody at 37 °C for 1 h. After washing, 3,3′-diaminobenzidine (DAB, ZLI-9017, ZSGB-BIO) was used to visualize immunoreactivity. All sections were then counterstained with hematoxylin to stain the nuclei. Finally, sections were dehydrated and mounted for microscopic examination.

For the TUNEL assay, retinal sections were deparaffinized and rehydrated. After rinsing with PBS, the sections were treated with proteinase K (Roche Applied Science, Indianapolis, IN) and quenched with 3% hydrogen peroxide; then they were incubated in a terminal deoxynucleotidyl transferase (TdT) reaction mix (Roche Applied Science) for 1 h at 37 °C. Sections were then incubated for 5 min with 4',6-diamidino-2-phenylindole (DAPI) at room temperature.

CircRNA enrichment and high-throughput sequencing: RNA was isolated using the RNeasy system (Qiagen, Dusseldorf, Germany), including on-column DNase I digestion (Qiagen) to eliminate DNA. Then the total RNA was depleted of ribosomal and linear RNA using the RiboMinus kit (Thermo Fisher Scientific, Waltham, MA) and RNase R (Epicenter, Madison, WI), respectively. CircRNAs were validated with quantitative reverse transcription (RT)–PCR using the VAHTSTM Library Quantification Kit (Vazyme Biotech Co., Ltd, Piscataway, NJ). Specifically, samples were heated to 70 °C for denaturing and then cooled to 40 °C on a thermocycler with RNase R buffer to digest linear RNA. After RNase R digestion and circRNA reverse transcription, the cDNA library was produced by PCR (conditions: 98 °C for 30 s, followed by 15 cycles of 98 °C for 10 s, 60 °C for 30 s, and 72 °C for 30 s, then 72 °C for 5 min) following depletion of the second cDNA chain with the USER enzyme. The sequencing libraries were constructed using the VAHTSTM Library Quantification Kit (Vazyme Biotech Co) and were sequenced with an Illumina HiSeq™ 2000 flowcell sequencer (Illumina, San Diego, CA).

Data analysis: The RNA-sequenced (RNA-seq) data were analyzed using FastQC software to verify the quality of the data [33]. The BWA-MEM alignment algorithm of the software BWA (the Burrows-Wheeler Alignment tool) was used to match the RNA-seq data to the genome [34]. To annotate the validated circRNAs, we used CIRI (CircRNA Identifier) software to predict the circRNAs [35] present in the sample and sequenced them using circBase [36]. The false discovery
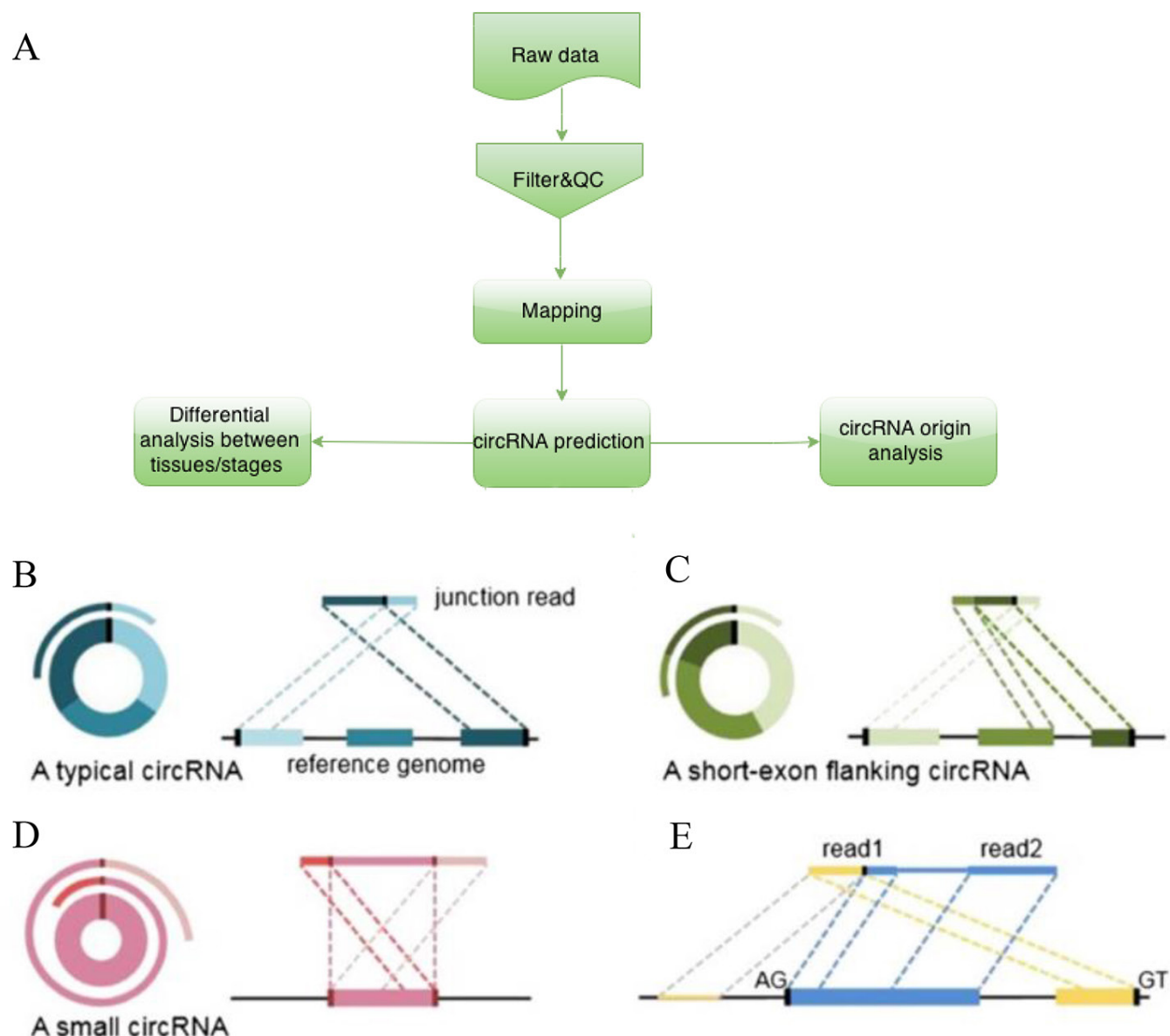
Figure 1. The basis and pipeline of circRNAs identification and analysis. **A**: After high throughput sequencing, raw data were collected and subsequently filtered and analyzed for quality control (QC). Clean data were mapped on the genome, and then the circular RNAs (circRNAs) were predicted via CIRI (CircRNA Identifier) and the circBase database. Finally, analyses of the differential expression between the time points, as well as function and origin analyses, were performed. **B**: Two segments of junction reads of classic circRNAs match to the relevant sequence in reverse orientation, albeit separately. **C**: If a flanking part of the junction is a short exon, the segment can align to the flanking exon of the circRNAs. **D**: If the circRNAs length is short, the read will possibly contain two terminal segments that align to the area of junction within circRNA. **E**: To reduce the false positive rate, candidate circRNAs are filtered via criteria as in a previous study.

rate (FDR) was used to correct for multiple hypothesis testing, and a twofold change and FDR≤0.001 was considered statistically significant [37]. Caspase-3-positive or TUNEL-positive cells were counted in a double-blinded manner from five discontinuous views randomly selected from each sample (n = 5 retinas). Data in the figures were analyzed with GraphPad Prism 5 software (GraphPad Software Inc., San Diego, CA)

and presented as mean ± standard error of the mean (SEM). A one-way ANOVA (ANOVA) followed by the Bonferroni correction, or the appropriate equivalent non-parametric test, was used for comparisons among groups, and a p-value of < 0.05 was denoted as statistically significant.

RESULTS

CircRNAs change during early development in the rat retina: We analyzed the raw reads or raw data of the expression of circRNA at P3, P7, and P12, using high-throughput sequencing followed by filtration and quality control (QC; Figure 1A, Table 1) to obtain clean reads as in a previous study [35]. Because exon–exon junction reads (Figure 1B-C) are important features of circRNAs that can map to the junction points of exons, the BWA software was used to match the clean reads to the genome and identify the junction reads. The results showed that the clean reads were expressed abundantly ($7–9 × 10^7$/group) and largely mapped to the genome (>75% of all reads) in the early developmental retina (Figure 2A, Table 2). Most of the clean reads mapped on the exon regions could be visualized at P7 (56.41% of all reads) but were present in only small amounts at P3 (15.21% of all reads) and P12 (17.78% of all reads; Figure 2A, Table 2). After the CIRI predictions and false-positive read filtration, validated circRNAs were obtained and annotated according to circBase (Figure 1E, Table 3, Appendix 1, Appendix 2 and Appendix 3).

To identify circRNA changes in the developing rat retina, the total circular junction reads of the different stages were further separated with BWA. CircRNAs with the same sequence were regarded as one circRNA species. The number of circular junction reads at P12 (143,815) was greater than that at P3 (78,758) and P7 (78,385), while the number of circRNA species at P7 (7,021) was greater than that at P3 (2,654) and P12 (5,628; Figure 2B, Table 4).

After the data were integrated, a total of 10,890 circRNAs were obtained; additionally, the overall expression of circRNAs was different among the P3, P7 and P12 time points. For example, there were 4,123 circRNAs expressed solely at P7 (Figure 2C). By comparing the expression of circRNA between the time points, we detected differential expression (greater than a twofold change, FDR≤0.001; Figure 3A,B, Appendix 4 and Appendix 5) of 1,371 circRNAs (out of 8,223 circRNAs) between P3 and P7 and 1,112 circRNAs (out of 10,016 circRNAs) between P7 and P12. We found that 558 circRNAs and 813 circRNAs (out of 1,371 circRNAs) were upregulated and downregulated, respectively, from P3 to P7. The circRNAs upregulated from P3 to P7 included those originating from the genes *Akt3*, *Ccdc6*, *Gnaz*, and *Mpped2*; the circRNAs downregulated from P3 to P7 originated from the genes *Ly6g6f*, *Melk*, *Casc5*, *Smarcc1*, and *Pank2* (Figure 3C, Appendix 4). We found that 434 or 678 circRNAs (out of 1,112 circRNAs) were upregulated or downregulated, respectively, from P7 to P12. Upregulated circRNAs included those derived from the genes *Pde6a*, *Unc13b*, *Pde4b*, *Pi4ka*, *Mtr*, and *Dnmbp*, while downregulated circRNAs included those derived from the genes *Pank2*, *Smarcc1*, *Melk*, *Ly6g6f*, *Casc5*, *Dst*, and *Pak3* (Figure 3D, Appendix 5). After the circRNAs expressed at only P3 or P12 were filtered out, a total of 438 circRNAs were retained for measuring significant changes in the circRNAs across the time points (Appendix 6, Figure 2D). Of these 438 circRNAs, ten were gradually downregulated, and 17 were gradually upregulated from day P3 to P12 (Appendix 7). In addition, 145 circRNAs were present in only small amounts or were undetectable (48 circRNAs) at P7 relative to P3 and P12. In addition, 266 circRNAs of the 438 circRNAs were present at P7 but were absent or diminished at P3 and P12 (172 circRNAs appeared only at P7, Figure 2D).

Physiologic neuronal apoptosis during early development in the rat retinal ganglion cell layer: Most neurons undergoing PCD exhibit the morphological and biochemical hallmarks of apoptosis, such as cell shrinkage, activation of caspases, and DNA fragmentation [5]. Cleaved caspase-3 is produced early in the apoptotic process and is responsible for executing the apoptotic process, making it a strong biomarker of apoptosis [38]. The TUNEL assay detects apoptosis by labeling the fragmented DNA generated during PCD. For enhanced reliability of the results, we used anti-cleaved caspase-3 immunohistochemistry and the TUNEL assay to detect apoptosis in retinas from rats at ages P3, P7, and P12. The cleaved caspase-3-positive-to-negative cell ratio increased from 1.69 ± 0.25% to 3.19 ± 0.42% between P3 and P7 (p = 0.005); it then decreased to 1.69 ± 0.25% between P7 and

TABLE 1. EXPRESSION, FILTRATION AND QUALITY CONTROL OF RAW DATA DURING EARLY DEVELOPMENT IN RAT RETINA.

Sample	Raw Reads	Clean reads	Raw data(G)	Clean data(G)	Error(%)	Q20(%)	Q30(%)
P3	96,172,040	79,680,804	14.43	11.95	0.03	96.91	92.68
P7	96,890,346	73,230,288	12.84	9.67	0.05	93.26	87.04
P12	104,779,880	89,480,408	15.72	13.42	0.02	97.41	93.56

Raw Reads: original sequence data. Clean reads: data after raw data filtration. Raw data: the number of original sequence multiplied by the length of the sequence. Clean data: the number of filtrated sequence multiplied by the length of the sequence. Error: base-rate error. Q20 Q30:ratio of bases with Phred quality score >20 or 30 in total base.
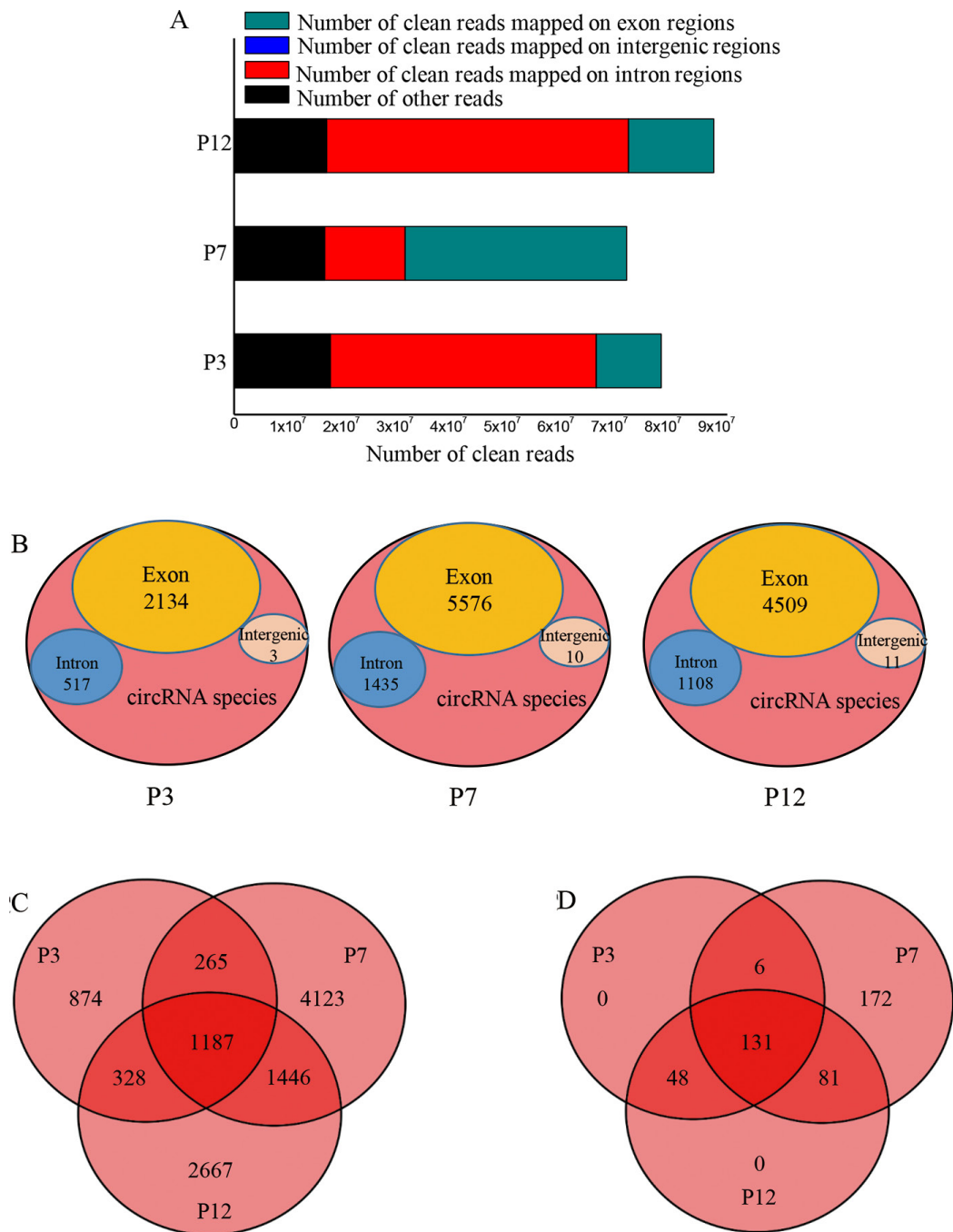
Figure 2. The expression of circRNA reads during postnatal development in the rat retina. **A**: Classification of the reads during early development in the rat retina. **B**: Classification of the origins of the circular RNA (circRNA) species during early development. **C**: Distribution of the total circRNA species at time points P3, P7, and P12. **D**: Distribution of the circRNA species after filtration (>twofold change, false discovery rate (FDR)≤0.001 for P3 versus P7 and P7 versus P12) at P3, P7, and P12.

TABLE 2. THE ORIGIN OF CLEAN READS IN DIFFERENT STAGE OF DEVELOPING RAT RETINA.

Sample	P3	P7	P12
Total number of clean reads	79,680,804	73,230,288	89,480,408
Number of clean reads mapped on genome	61,697,391 (77.43%)	56,325,618 (76.92%)	72,183,843 (80.67%)
Number of clean reads mapped on intron regions	49,562,407 (62.20%)	15,004,813 (20.49%)	56,256,016 (62.87%)
Number of clean reads mapped on intergenic regions	19,376 (0.02%)	11,008 (0.02%)	15,521 (0.02%)
Number of clean reads mapped on exon regions	12,115,608 (15.21%)	41,309,797 (56.41%)	15,912,306 (17.78%)

The number of clean reads in P3, P7 and P12 rat retina and the clean reads origination such as exon regions, intron regions or intergenic regions.

TABLE 3. THE ANNOTATION OF CIRCRNA.

circRNA_ID	Chr	circRNA_start	circRNA_end	#junction reads	#non_junction reads	CircRNAs type	gene_ID
chr1:1901431|1901647	Chr1	1,901,431	1,901,647	5	34	exon	Ppil4
chr1:1901431|1909369	Chr1	1,901,431	1,909,369	5	22	exon	Ppil4
chr1:2375315|2377265	Chr1	2,375,315	2,377,265	7	7	exon	Ust
chr1:2839790|2849731	Chr1	2,839,790	2,849,731	2	8	intron	SNORA32
chr1:3879152|3915233	Chr1	3,879,152	3,915,233	5	79	exon	Stxbp5

circRNA_ID: code of circRNAs. Chr: host chromosome of circRNAs. circRNA_start and circRNA_end: the starting and ending location of circRNA in host chromosome. #junction reads: number of junction reads formed by back-splicing #non_junction_reads: number of reads which mapped on the flanking area of the head and tail end. CircRNA type: the head and tail end of circRNAs that could be both mapped on the exon area belong to exon type, otherwise belong to intron type. gene_ID: corresponding host gene code of circRNAs according to the location information.

TABLE 4. THE EXPRESSION OF CIRCRNAS IN DIFFERENT STAGE OF DEVELOPING RAT RETINA.

Sample	P3	P7	P12
Number of circular junction reads	78,758	78,385	143,815
Number of circRNA species	2,654	7,021	5,628
Number of circRNA species originated from exon regions	2,134 (80.41%)	5,576 (79.42%)	4,509 (80.12%)
Number of circRNA species originated from intron regions	517 (19.48%)	1,435 (20.44%)	1,108 (19.69%)
Number of circRNA species originated from intergenic regions	3 (0.11%)	10 (0.14%)	11 (0.20%)

The expression of circular junction reads and circRNAs species in P3, P7 and P12 rat retina. And the expression of circRNAs origination such as exon regions, intron regions or intergenic regions.
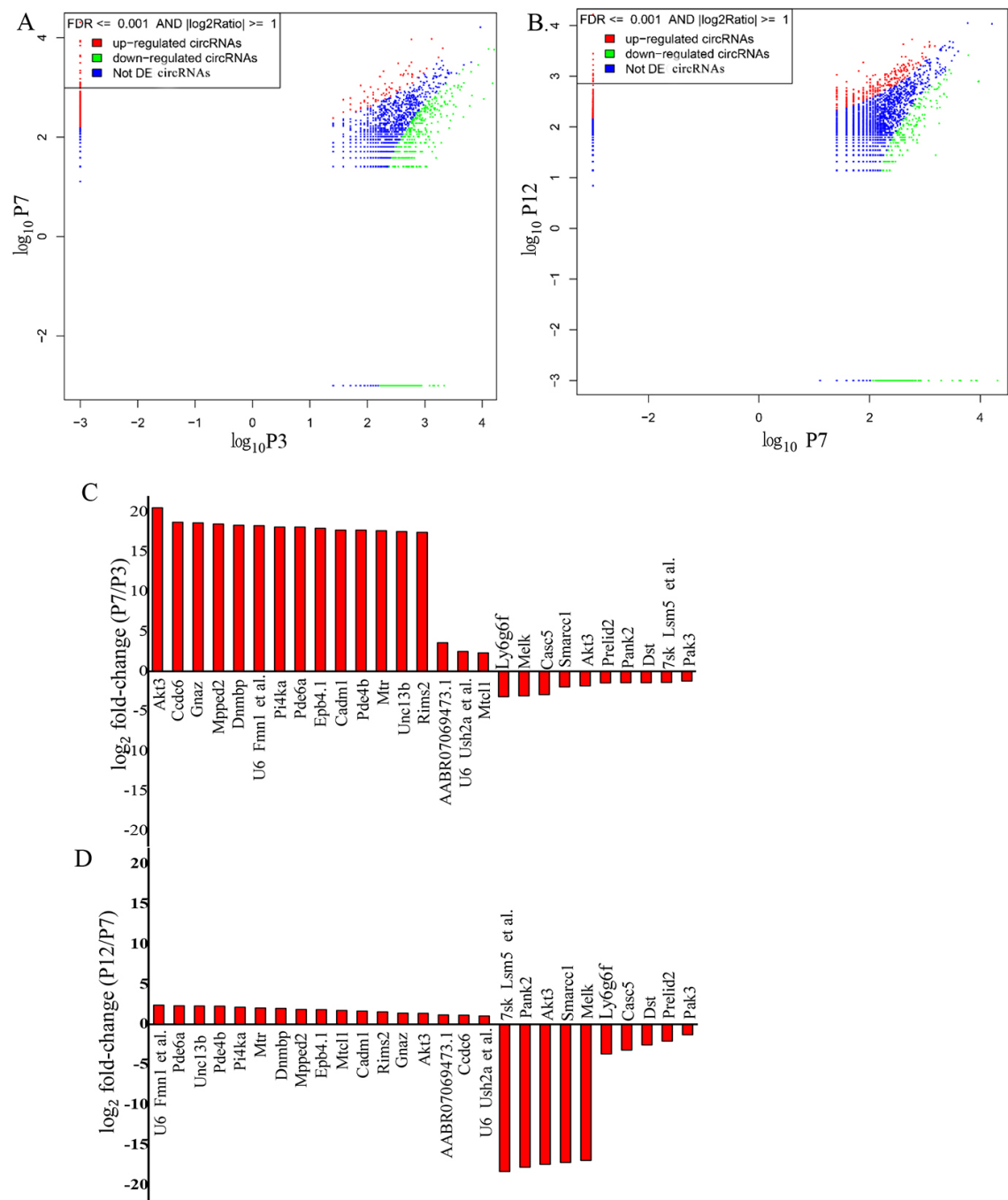
Figure 3. The changes in circRNAs during postnatal development in the rat retina. **A**, **B**: Expression profile of circular RNAs (circRNAs) in the early developing rat retina between P3 and P7, and P7 and P12, respectively. **C**, **D**: Bar graphs showing the expression changes in the circRNAs from P3 to P7 and P7 to P12, respectively.

P12 (p = 0.008; Figure 4A,C). The TUNEL-positive cell ratio increased from 6.75 ± 0.88% to 12.77 ± 1.17% between P3 and P7 (p<0.001) and then decreased to 7.16 ± 0.62% between P7 and P12 (p<0.001; Figure 4B,D). The results confirmed that normal age-dependent physiologic apoptosis of neurons was occurring.

Candidate circRNAs from host genes associated with apoptosis: We identified changes in the expression of circRNA that could be linked to normal developmental apoptosis during in the neonatal rat retina. A total of 15 circRNAs from genes associated with apoptosis were obtained after further filtration and screening (Table 5). We found that five
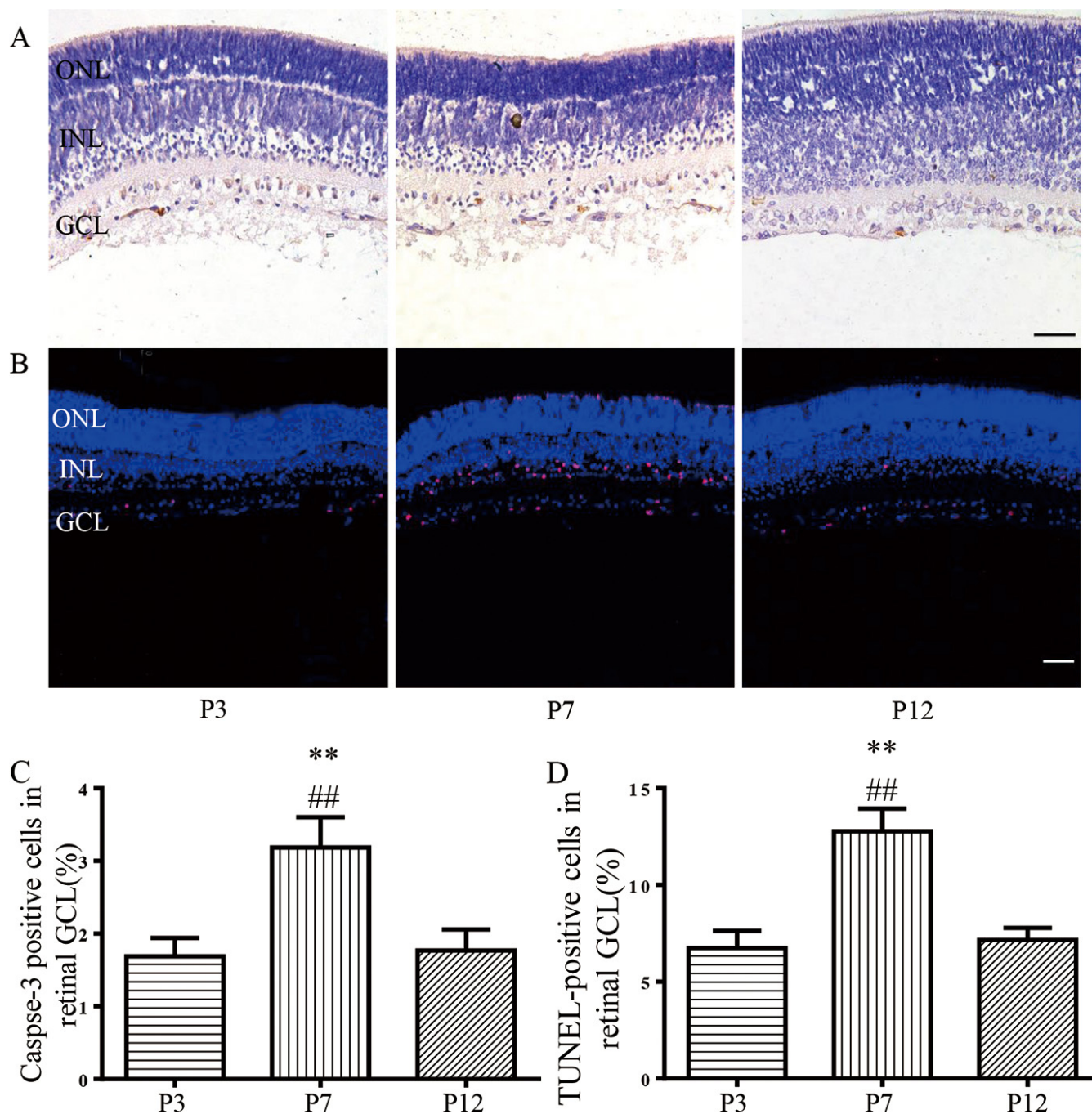
Figure 4. Physiologic neuronal apoptosis occurred in an age-dependent manner during the postnatal development of the rat retina. Neuronal apoptosis of rat retinas was detected with cleaved caspase-3 immunolabeling (cleaved caspase-3-positive) and with the terminal deoxynucleotidyl transferase dUTP nick end labeling (TUNEL) assay (TUNEL-positive; n = 5 retinas per group). **A**: Representative photomicrograph of caspase-3-positive cells (brown) in the rat retinal GCL. Scale bar = 50 μm. **B**: Respective photomicrograph of TUNEL-positive cells (red) in the rat retinal GCL. Scale bar = 25 μm. **C**: The mean percentages of caspase-3 positive cells at P3, P7, and P12. **D**: The percentages of TUNEL-positive cells in the retinal GCL. #$p<0.05$, ##$p<0.01$ versus P3, #$p<0.05$, ##$p<0.01$ versus P12. One-way ANOVA followed by Bonferroni's post-hoc test. ONL, outer nuclear layer; INL, inner nuclear layer; GCL, ganglion cell layer.

circRNAs (from the genes *Optn*, *Thoc1*, *Rbm5*, *Ddx19a*, and *Bnip2*) could not be detected, and two circRNAs (from the genes *Pias1* and *Naa35*) were not expressed at P7 but were abundantly expressed at P3 and P12. Three circRNAs (from the genes *Rere*, *Arhgap10*, and *Birc6*) were expressed specifically at P7, and three circRNAs (from the genes *Ranbp9*, *Epha7*, and *Braf*) could be visualized at P7 but were absent or diminished at P3 and P12 (Figure 5).

DISCUSSION

In this study, we explored physiologic neuronal apoptosis and the expression of circRNAs during early development in the rat retina. Hundreds of circRNAs were abundantly and differentially expressed during the early development of the rat retina. Expression of circRNA followed several patterns: 1) stage-specific expression or suppression, 2) gradual increases or decreases between time points, or 3) stable expression at all stages of early development. We confirmed age-dependent physiologic neuronal apoptosis was occurring in the developing rat retina. In addition, circRNAs originated from genes that were associated with apoptosis (such as *Thoc1*, *Akt3*, *Rere*, *Rbm5*, *Ranbp9*, *Pias1*, *Optn*, *Naa35*, *Melk*, *Epha7*, *Ddx19a*, *Braf*, *Bnip2*, *Birc6*, and *Arhgap10*) changed dramatically in the developing rat retina, suggesting a link between circRNA and physiologic neuronal apoptosis.

Numerous changes in the nervous system occur during the period of peak developmental apoptosis (P4 to P14) [9,10]. For example, the *N*-Methyl-D-aspartate (NMDA) receptor intracellular signaling pathway switches from the ERK1/2 to the p38 mitogen-activated protein kinase pathway [14]. CircRNA is non-coding RNA mainly composed of exons and is abundant in eukaryotic cells, with highly conserved spatiotemporal specificity [25,26,39]. Several studies have shown that circRNAs are associated with physiologic and pathological processes, such as development of the nervous system [28,40], atherosclerosis [27,41], and cancer [42-44]. The present data indicate that circRNAs may play an important role in the development of the rat retina.

According to these results, apoptosis increased to a peak at or near P7 in the developing rat retinal ganglion cell layer [11]. Although the mechanisms underlying circRNA function are not well-known, studies by Hansen et al. and Memczak et al. showed that circRNA participates in post-transcriptional regulation by acting as a miRNA sponge, interfering with cognate linear isoforms [28,29,42]. In addition, researchers showed that circRNA can bind with Argonaute proteins [29] or RNA-binding proteins, or can base-pair with other RNAs [45,46], to interfere with the transcription and translation of mRNA. Some circRNAs can even produce proteins [47].

Through a bioinformatics analysis of circRNAs at different ages of the developing rat retina, the expression of circRNA in 15 circRNAs originating from genes associated with apoptosis was found to change over time. Previous studies have showed large numbers of circRNAs that are endogenous to mammalian cells, and many of these circRNAs are much more stable than linear RNAs [30, 48]; therefore, we believe the observed differences in the expression of transcripts per million (TPM) of the candidate circRNAs were mostly validated rather than simply caused by outliers. As circRNAs can interfere with their cognate linear RNAs, these circRNAs may be linked to physiologic neuronal apoptosis in the developing retina. For example, the *Pias1 gene* (also known as *STAT1*) encodes a protein involved in the G1/S transition of the mitotic cell cycle and is a negative regulator of apoptotic processes. The miRNA rno-miR-204-3p is one of the predicted targets of circRNA from Pias1; upregulation of this miRNA induces glioma cell apoptosis [49]. The present study detected low expression of the circRNA from this gene at P7, which may lead to high levels of this miRNA and silencing or cleavage of its cognate mRNA, thus facilitating the apoptotic process. In another example, the *Rere gene* encodes a member of the atrophin family of arginine-glutamic acid dipeptide repeat-containing proteins; this protein colocalizes with a transcription factor

TABLE 5. CANDIDATE CIRCRNAS AND THE HOST GENE MAY LINK TO NEURONAL PHYSIOLOGIC APOPTOSIS.

circRNA_ID	Gene_ID
chr17:77176705|77178100	Optn
chr18:1164675|1169033	Thoc1
chr8:116505048|116505353	Rbm5
chr19:43254907|43259022	Ddx19a
chr8:76405782|76406571	Bnip2
chr8:67801800|67812158	Pias1
chr17:5429865|5436758	Naa35
chr5:167486007|167558256	Rere
chr19:34233020|34253181	Arhgap10
chr6:22033342|22038870	Birc6
chr17:24052253|24058139	Ranbp9
chr5:43659900|43661144	Epha7
chr4:67449579|67450836	Braf
chr13:95193009|95196402	Akt3
chr5:59831651|59833591	Melk

The circRNA_ID of candidate circRNAs and the corresponding host gene.

in the nucleus that triggers apoptosis when overexpressed. Notably, overexpression of Rere-derived circRNA may absorb (sponge) rno-miR-128-3p miRNA, which may result in overexpression of the relevant protein (Mapk14, a proapoptotic protein) and subsequent apoptosis [50]. Thus, we believe that the identified circRNAs are potentially important to the processes of physiologic neuronal apoptosis during maturation of the nervous system, acting as microRNA sponges or through other mechanisms mentioned above.

The present study has the following limitations. We did not precisely classify the data or screen other circRNAs that may be related to apoptosis, nor did we verify the candidate circRNAs and their specific effects in physiologic neuronal apoptosis. In addition, we did not analyze the expression

patterns of the host genes of the candidate circRNAs, and their effects on microRNA or mRNA, and the expression profiles of the circRNAs in the adult retina. Such studies should be performed in the future. However, we did predict possible functions or pathways through Gene Ontology (GO) enrichment analysis, pathway enrichment analysis, and miRNA-binding target prediction (data not shown), which provide fertile areas for further study.

In conclusion, we confirmed the temporal dependence of developmental physiologic neuronal apoptosis and found 15 circRNAs that had significant differential expression patterns and may be involved in developmental apoptosis. As the nervous system is highly vulnerable to ethanol, general anesthetics, and other substances during this postnatal
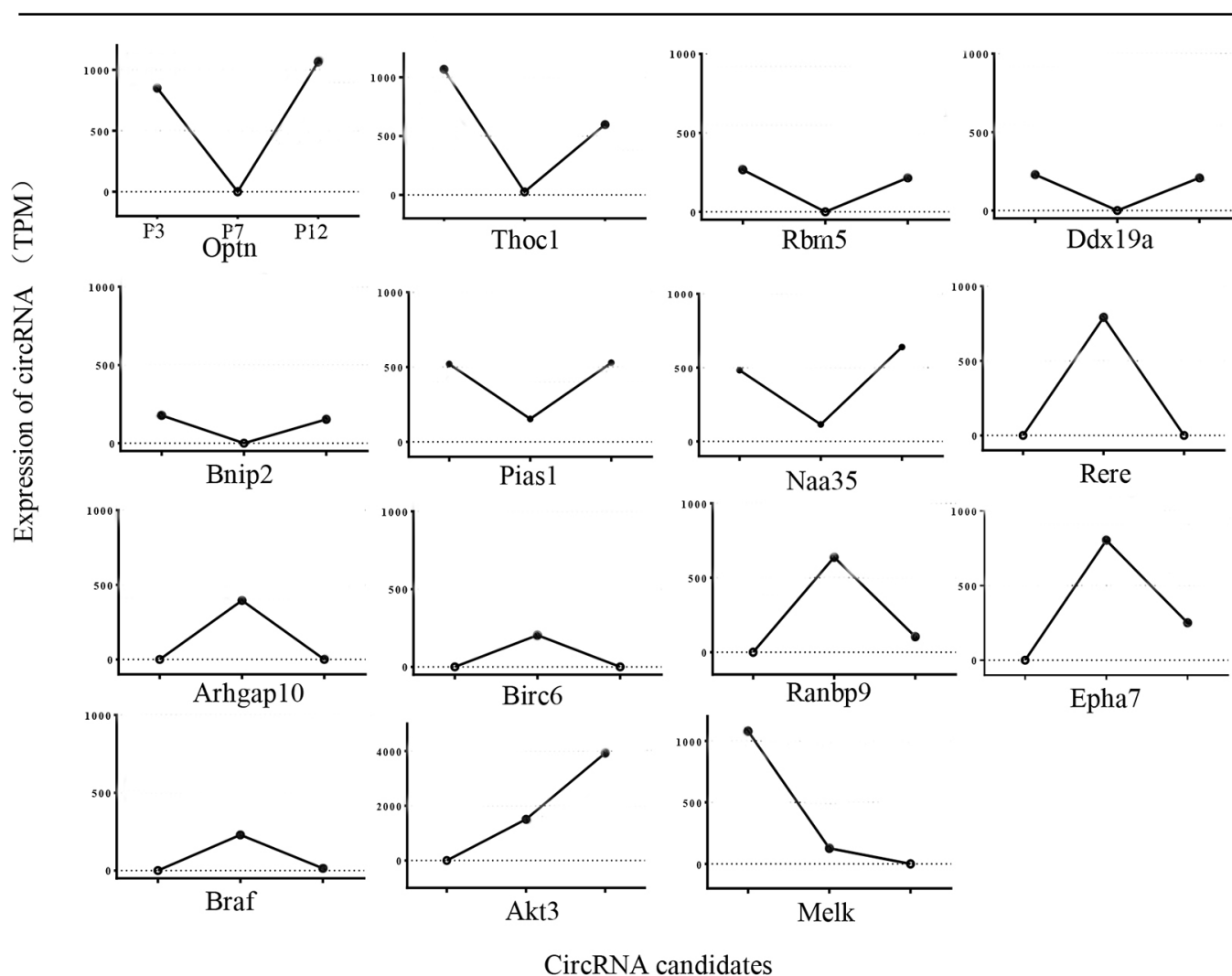

Figure 5. Expression changes in candidate circRNAs derived from apoptosis-related genes during postnatal development in the rat retina. The number of circular junction reads of a circular RNA (circRNA) was normalized to get the transcripts per million (TPM) that was used to compare the expression of circRNAs between groups. The TPM is used as the unit of the y-axis. Dotted lines represent the "y=0" line, and the open circles on the dotted lines mean that the circRNA candidates were not detected.

developmental period, these results may offer potential mechanisms for regulating drug-induced apoptosis in the nervous system.

APPENDIX 1. ANNOTATION OF P3 RAT RETINA CIRCRNAS

To access the data, click or select the words "Appendix 1."

APPENDIX 2. ANNOTATION OF P7 RAT RETINA CIRCRNAS

To access the data, click or select the words "Appendix 2."

APPENDIX 3. ANNOTATION OF P12 RAT RETINA CIRCRNAS

To access the data, click or select the words "Appendix 3."

APPENDIX 4. CHANGE OF CIRCRNAS BETWEEN P3 AND P7 IN RAT RETINA.

To access the data, click or select the words "Appendix 4." Comparison of circRNAs between P3 and P7 in rat retina. circRNA_ID: code of circRNAs. gene_ID: corresponding host gene code of circRNAs. Expression: number of circular junction reads that were formed by back splicing. TPM: circular junction reads of a circRNAwas normalized to get a "TPM (Transcripts per million)" before comparison between groups. Fold-change: change of circRNAs between groups. FDR: False discovery rate (FDR) was used to rectify the multiple hypothesis testing of P-value, and a two-fold change and FDR ≤0.001 was denoted as statistically significant.

APPENDIX 5. CHANGE OF CIRCRNAS BETWEEN P7 AND P12 IN RAT RETINA.

To access the data, click or select the words "Appendix 5." Comparison of circRNAs between P7 and P12 in rat retina. circRNA_ID: code of circRNAs.gene_ID: corresponding host gene code of circRNAs. Expression: number of circular junction reads that were formed by back splicing. TPM: circular junction reads of a circRNA was normalized to get a "TPM (Transcripts per million)" before comparison between groups. Fold-change: change of circRNAs between groups. FDR: False discovery rate (FDR) was used to rectify the multiple hypothesis testing of P-value, and a two-fold change and FDR ≤0.001 was denoted as statistically significant.

APPENDIX 6. CHANGE OF CIRCRNAS BETWEENP3, P7 AND P12 IN RAT RETINA.

To access the data, click or select the words "Appendix 6." circRNA_ID: code of circRNAs. gene_ID: corresponding host gene code of circRNAs. TPM: circular junction reads of a circRNA was normalized to get a "TPM (Transcripts per million)" before comparison between groups. Fold-change: change of circRNAs between groups. FDR: False discovery rate (FDR) was used to rectify the multiple hypothesis testing of P-value, and a two-fold change and FDR ≤0.001 was denoted as statistically significant.

APPENDIX 7. CIRCRNAS BETWEENP3, P7 AND P12 IN RAT RETINA

To access the data, click or select the words "Appendix 7." Change gradually. circRNA_ID: code of circRNAs. gene_ID: corresponding host gene code of circRNAs. TPM: circular junction reads of a circRNA was normalized to get a "TPM (Transcripts per million)" before comparison between groups. Fold-change: change of circRNAs between groups. FDR: False discovery rate (FDR) was used to rectify the multiple hypothesis testing of P-value, and a two-fold change and FDR ≤0.001 was denoted as statistically significant.

REFERENCES

1. Voyvodic JT. Cell death in cortical development: How much? Why? So what? Neuron 1996; 16:693-6. [PMID: 8607987].

2. Danial NN, Korsmeyer SJ. Cell death: critical control points. Cell 2004; 116:205-19. [PMID: 14744432].

3. Young RW. Cell death during differentiation of the retina in the mouse. J Comp Neurol 1984; 229:362-73. [PMID: 6501608].

4. Livesey FJ, Cepko CL. Vertebrate neural cell-fate determination: lessons from the retina. Nat Rev Neurosci 2001; 2:109-18. [PMID: 11252990].

5. Kim WR, Sun W. Programmed cell death during postnatal development of the rodent nervous system. Dev Growth Differ 2011; 53:225-35. [PMID: 21338348].

6. Creeley CE, Olney JW. Drug-Induced Apoptosis: Mechanism by which Alcohol and Many Other Drugs Can Disrupt Brain Development. Brain Sci 2013; 3:1153-81. [PMID: 24587895].

7. Yon JH, Daniel-Johnson J, Carter LB, Jevtovic-Todorovic V. Anesthesia induces neuronal cell death in the developing rat brain via the intrinsic and extrinsic apoptotic pathways. Neuroscience 2005; 135:815-27. [PMID: 16154281].

8. Cheng Y, He L, Prasad V, Wang S, Levy RJ. Anesthesia-Induced Neuronal Apoptosis in the Developing Retina: A Window of Opportunity. Anesth Analg 2015; 121:1325-35. [PMID: 26465931].

9. Ikonomidou C, Bosch F, Miksa M, Bittigau P, Vockler J, Dikranian K, Tenkova TI, Stefovska V, Turski L, Olney JW. Blockade of NMDA receptors and apoptotic neurodegeneration in the developing brain. Science 1999; 283:70-4. [PMID: 9872743].

10. Syed MM, Lee S, Zheng J, Zhou ZJ. Stage-dependent dynamics and modulation of spontaneous waves in the developing rabbit retina. J Physiol 2004; 560:533-49. [PMID: 15308679].

11. Dong J, Gao L, Han J, Zhang J, Zheng J. Dopamine Attenuates Ketamine-Induced Neuronal Apoptosis in the Developing Rat Retina Independent of Early Synchronized Spontaneous Network Activity. Mol Neurobiol 2016; [PMID: 27177547].

12. Motti D, Bixby JL, Lemmon VP. MicroRNAs and neuronal development. Semin Fetal Neonatal Med 2012; 17:347-52. [PMID: 22906916].

13. Doubi-Kadmiri S, Benoit C, Benigni X, Beaumont G, Vacher CM, Taouis M, Baroin-Tourancheau A, Amar L. Substantial and robust changes in microRNA transcriptome support postnatal development of the hypothalamus in rat. Sci Rep 2016; 6:24896-[PMID: 27118433].

14. Xiao L, Hu C, Feng C, Chen Y. Switching of N-methyl-D-aspartate (NMDA) receptor-favorite intracellular signal pathways from ERK1/2 protein to p38 mitogen-activated protein kinase leads to developmental changes in NMDA neurotoxicity. J Biol Chem 2011; 286:20175-93. [PMID: 21474451].

15. Kaindl AM, Koppelstaetter A, Nebrich G, Stuwe J, Sifringer M, Zabel C, Klose J, Ikonomidou C. Brief alteration of NMDA or GABAA receptor-mediated neurotransmission has long term effects on the developing cerebral cortex. Molecular & cellular proteomics MCP 2008; 7:2293-310. [PMID: 18587059].

16. Dajas-Bailador F, Bonev B, Garcez P, Stanley P, Guillemot F, Papalopulu N. microRNA-9 regulates axon extension and branching by targeting Map1b in mouse cortical neurons. Nat Neurosci 2012; [PMID: 22484572].

17. Shibata M, Nakao H, Kiyonari H, Abe T, Aizawa S. MicroRNA-9 regulates neurogenesis in mouse telencephalon by targeting multiple transcription factors. J Neurosci 2011; 31:3407-22. [PMID: 21368052].

18. Han Z, Chen F, Ge X, Tan J, Lei P, Zhang J. miR-21 alleviated apoptosis of cortical neurons through promoting PTEN-Akt signaling pathway in vitro after experimental traumatic brain injury. Brain Res 2014; 1582:12-20. [PMID: 25108037].

19. Cui C, Xu G, Qiu J, Fan X. Up-regulation of miR-26a promotes neurite outgrowth and ameliorates apoptosis by inhibiting PTEN in bupivacaine injured mouse dorsal root ganglia. Cell Biol Int 2015; 39:933-42. [PMID: 25808510].

20. Chen Q, Xu J, Li L, Li H, Mao S, Zhang F, Zen K, Zhang CY, Zhang Q. MicroRNA-23a/b and microRNA-27a/b suppress Apaf-1 protein and alleviate hypoxia-induced neuronal apoptosis. Cell Death Dis 2014; 5:e1132-[PMID: 24651435].

21. Qi Y, Zhang M, Li H, Frank JA, Dai L, Liu H, Chen G. MicroRNA-29b regulates ethanol-induced neuronal apoptosis in the developing cerebellum through SP1/RAX/PKR cascade. J Biol Chem 2014; 289:10201-10. [PMID: 24554719].

22. Nigro JM, Cho KR, Fearon ER, Kern SE, Ruppert JM, Oliner JD, Kinzler KW, Vogelstein B. Scrambled exons. Cell 1991; 64:607-13. [PMID: 1991322].

23. Kos A, Dijkema R, Arnberg AC, van der Meide PH, Schellekens H. The hepatitis delta (delta) virus possesses a circular RNA. Nature 1986; 323:558-60. [PMID: 2429192].

24. Danan M, Schwartz S, Edelheit S, Sorek R. Transcriptome-wide discovery of circular RNAs in Archaea. Nucleic Acids Res 2012; 40:3131-42. [PMID: 22140119].

25. Salzman J, Gawad C, Wang PL, Lacayo N, Brown PO. Circular RNAs are the predominant transcript isoform from hundreds of human genes in diverse cell types. PLoS One 2012; 7:e30733-[PMID: 22319583].

26. Jeck WR, Sorrentino JA, Wang K, Slevin MK, Burd CE, Liu J, Marzluff WF, Sharpless NE. Circular RNAs are abundant, conserved, and associated with ALU repeats. RNA 2013; 19:141-57. [PMID: 23249747].

27. Salzman J, Chen RE, Olsen MN, Wang PL, Brown PO. Cell-type specific features of circular RNA expression. PLoS Genet 2013; 9:e1003777-[PMID: 24039610].

28. Memczak S, Jens M, Elefsinioti A, Torti F, Krueger J, Rybak A, Maier L, Mackowiak SD, Gregersen LH, Munschauer M, Loewer A, Ziebold U, Landthaler M, Kocks C, le Noble F, Rajewsky N. Circular RNAs are a large class of animal RNAs with regulatory potency. Nature 2013; 495:333-8. [PMID: 23446348].

29. Hansen TB, Jensen TI, Clausen BH, Bramsen JB, Finsen B, Damgaard CK, Kjems J. Natural RNA circles function as efficient microRNA sponges. Nature 2013; 495:384-8. [PMID: 23446346].

30. Rybak-Wolf A, Stottmeister C, Glazar P, Jens M, Pino N, Giusti S, Hanan M, Behm M, Bartok O, Ashwal-Fluss R, Herzog M, Schreyer L, Papavasileiou P, Ivanov A, Ohman M, Refojo D, Kadener S, Rajewsky N. Circular RNAs in the Mammalian Brain Are Highly Abundant, Conserved, and Dynamically Expressed. Mol Cell 2015; 58:870-85. [PMID: 25921068].

31. You X, Vlatkovic I, Babic A, Will T, Epstein I, Tushev G, Akbalik G, Wang M, Glock C, Quedenau C, Wang X, Hou J, Liu H, Sun W, Sambandan S, Chen T, Schuman EM, Chen W.

Neural circular RNAs are derived from synaptic genes and regulated by development and plasticity. Nat Neurosci 2015; 18:603-10. [PMID: 25714049].

32. Kadam RS, Williams J, Tyagi P, Edelhauser HF, Kompella UB. Suprachoroidal delivery in a rabbit ex vivo eye model: influence of drug properties, regional differences in delivery, and comparison with intravitreal and intracameral routes. Mol Vis 2013; 19:1198-210. [PMID: 23734089].

33. Kroll KW, Mokaram NE, Pelletier AR, Frankhouser DE, Westphal MS, Stump PA, Stump CL, Bundschuh R, Blachly JS, Yan P. Quality Control for RNA-Seq (QuaCRS): An Integrated Quality Control Pipeline. Cancer Inform 2014; 13:Suppl 37-14. [PMID: 25368506].

34. Li H. Aligning sequence reads, clone sequences and assembly contigs with BWA-MEM. Genomics 2013; xxx:3997-.

35. Gao Y, Wang J, Zhao F. CIRI: an efficient and unbiased algorithm for de novo circular RNA identification. Genome Biol 2015; 16:4-[PMID: 25583365].

36. Glazar P, Papavasileiou P, Rajewsky N. circBase: a database for circular RNAs. RNA 2014; 20:1666-70. [PMID: 25234927].

37. Ren S, Peng Z, Mao JH, Yu Y, Yin C, Gao X, Cui Z, Zhang J, Yi K, Xu W, Chen C, Wang F, Guo X, Lu J, Yang J, Wei M, Tian Z, Guan Y, Tang L, Xu C, Wang L, Gao X, Tian W, Wang J, Yang H, Wang J, Sun Y. RNA-seq analysis of prostate cancer in the Chinese population identifies recurrent gene fusions, cancer-associated long noncoding RNAs and aberrant alternative splicings. Cell Res 2012; 22:806-21. [PMID: 22349460].

38. Vecino E, Hernandez M, Garcia M. Cell death in the developing vertebrate retina. Int J Dev Biol 2004; 48:965-74. [PMID: 15558487].

39. Cocquerelle C, Mascrez B, Hetuin D, Bailleul B. Mis-splicing yields circular RNA molecules. FASEB J 1993; 7:155-60. [PMID: 7678559].

40. Hansen TB, Wiklund ED, Bramsen JB, Villadsen SB, Statham AL, Clark SJ, Kjems J. miRNA-dependent gene silencing involving Ago2-mediated cleavage of a circular antisense RNA. EMBO J 2011; 30:4414-22. [PMID: 21964070].

41. Burd CE, Jeck WR, Liu Y, Sanoff HK, Wang Z, Sharpless NE. Expression of linear and novel circular forms of an INK4/ARF-associated non-coding RNA correlates with atherosclerosis risk. PLoS Genet 2010; 6:e1001233-[PMID: 21151960].

42. Hansen TB, Kjems J, Damgaard CK. Circular RNA and miR-7 in cancer. Cancer Res 2013; 73:5609-12. [PMID: 24014594].

43. Bachmayr-Heyda A, Reiner AT, Auer K, Sukhbaatar N, Aust S, Bachleitner-Hofmann T, Mesteri I, Grunt TW, Zeillinger R, Pils D. Correlation of circular RNA abundance with proliferation–exemplified with colorectal and ovarian cancer, idiopathic lung fibrosis, and normal human tissues. Sci Rep 2015; 5:8057-[PMID: 25624062].

44. Wang X, Zhang Y, Huang L, Zhang J, Pan F, Li B, Yan Y, Jia B, Liu H, Li S, Zheng W. Decreased expression of hsa_circ_001988 in colorectal cancer and its clinical significances. Int J Clin Exp Pathol 2015; 8:16020-5. [PMID: 26884878].

45. Wilusz JE, Sharp PA. Molecular biology. A circuitous route to noncoding RNA. Science 2013; 340:440-1. [PMID: 23620042].

46. Tay Y, Rinn J, Pandolfi PP. The multilayered complexity of ceRNA crosstalk and competition. Nature 2014; 505:344-52. [PMID: 24429633].

47. Chen CY, Sarnow P. Initiation of protein synthesis by the eukaryotic translational apparatus on circular RNAs. Science 1995; 268:415-7. [PMID: 7536344].

48. Jeck WR, Sharpless NE. Detecting and characterizing circular RNAs. Nat Biotechnol 2014; 32:453-61. [PMID: 24811520].

49. Chen PH, Chang CK, Shih CM, Cheng CH, Lin CW, Lee CC, Liu AJ, Ho KH, Chen KC. The miR-204–3p-targeted IGFBP2 pathway is involved in xanthohumol-induced glioma cell apoptotic death. Neuropharmacology 2016; 110:362-75. .

50. Mao G, Ren P, Wang G, Yan F, Zhang Y. MicroRNA-128–3p Protects Mouse Against Cerebral Ischemia Through Reducing p38alpha Mitogen-Activated Protein Kinase Activity. J Mol Neurosci 2017; 61:152-8. .